

## Ag<sub>4</sub>L<sub>2</sub> Nanocage as a Building Unit toward the Construction of Silver Metal Strings

Jing-Yun Wu,<sup>†</sup> Yu-Fang Lin,<sup>†,‡</sup> Chuan-Hung Chuang,<sup>†</sup> Tien-Wen Tseng,<sup>‡</sup> Yuh-Sheng Wen,<sup>†</sup> and Kuang-Lieh Lu<sup>\*,†</sup>

Institute of Chemistry, Academia Sinica, Taipei 115, Taiwan, and Department of Chemical Engineering, National Taipei University of Technology, Taipei 106, Taiwan

Received May 14, 2008

Self-assembly of AgNO<sub>3</sub> with the semirigid tetratopic ligands 1,2,4,5-tetrakis(benzoimidazol-1-ylmethyl)benzene (TBim) and 1,2,4,5-tetrakis(5,6-dimethylbenzimidazol-1-ylmethyl)benzene (TDMBim) afforded compounds [Ag<sub>4</sub>(μ<sub>4</sub>-TBim)<sub>2</sub>(μ<sub>2</sub>-η<sup>2</sup>-NO<sub>3</sub>)<sub>2</sub>](NO<sub>3</sub>)<sub>2</sub> · 1/2CH<sub>2</sub>Cl<sub>2</sub> · 2CH<sub>3</sub>OH (1) and [(NO<sub>3</sub><sup>-</sup>)<sub>2</sub>][Ag<sub>4</sub>(μ<sub>4</sub>-TDMBim)<sub>2</sub>][Ag(NO<sub>3</sub>)<sub>2</sub>](NO<sub>3</sub>)<sub>2</sub> · CH<sub>2</sub>Cl<sub>2</sub> · CH<sub>3</sub>OH · 4H<sub>2</sub>O (2 · CH<sub>2</sub>Cl<sub>2</sub> · CH<sub>3</sub>OH · 4H<sub>2</sub>O), respectively. The structures of **1** and **2** were characterized by single-crystal X-ray diffraction analysis. Both compounds adopt a M<sub>4</sub>L<sub>2</sub>-type tetragonal metalloprismatic cage structure, [Ag<sub>4</sub>(μ<sub>4</sub>-L)<sub>2</sub>]<sup>4+</sup>, with strong intramolecular silver–silver contacts. Compound **1** is a discrete species, while compound **2** is a novel infinite chainlike supramolecular array involving silver metal strings assembled from a [Ag<sub>4</sub>(μ<sub>4</sub>-L)<sub>2</sub>]<sup>4+</sup> nanocage and silver linkages. Thermogravimetric analyses of 1 · 1/2CH<sub>2</sub>Cl<sub>2</sub> · 2CH<sub>3</sub>OH and 2 · CH<sub>3</sub>OH · 4H<sub>2</sub>O indicate that the Ag<sub>4</sub>L<sub>2</sub>-cage structures of **1** and **2** both are thermally stable up to 330 °C. Results from an in situ <sup>1</sup>H NMR study of AgNO<sub>3</sub> and TDMBim in different molar ratios unambiguously revealed the successive self-organization process, in which self-organization of the molecular cage takes place initially followed by crystallization of the corresponding supramolecular arrays with silver metal strings.

### Introduction

Self-organization is an essential process for progressively unraveling of the complexity of living organisms, biominerals, and supramolecular materials.<sup>1,2</sup> Information-directed generation of discrete, organized, and functional supramolecular entities from relatively simple molecular components by metal coordination is an intense area of investigation at the forefront of supramolecular chemistry.<sup>3–14</sup> The underlying principle of self-assembly resides in suitably designed, information-encoded metallocorners such as *cis*-[M(en)]<sup>2+</sup> (M = Pd, Pt),<sup>5</sup> *cis*-[Pt(phosphine)<sub>2</sub>]<sup>2+</sup>,<sup>4</sup> and *fac*-(CO)<sub>3</sub>-ReX,<sup>15–17</sup> etc., as building blocks to fulfill the requirements for recognition, orientation, and termination during the highly

precise assembly process.<sup>18</sup> Interestingly, this strategy applies to a unique type of complex matter that involves ligand-supported and/or ligand-unsupported one-dimensional oli-

\* To whom correspondence should be addressed. E-mail: lu@chem.sinica.edu.tw. Fax: +886-2-27831237.

<sup>†</sup> Academia Sinica.

<sup>‡</sup> National Taipei University of Technology.

- (1) (a) Lehn, J.-M. *Supramolecular Chemistry: Concepts and Perspectives*; VCH: Weinheim, Germany, 1995. (b) Lehn, J.-M. *Proc. Natl. Acad. Sci. U.S.A.* **2002**, *99*, 4763.
- (2) Davis, A. V.; Yeh, R. M.; Raymond, K. N. *Proc. Natl. Acad. Sci. U.S.A.* **2002**, *99*, 4793.
- (3) (a) Baxter, P. N. W.; Lehn, J.-M.; Baum, G.; Fenske, D. *Chem.—Eur. J.* **1999**, *5*, 102. (b) Abrahams, B. F.; Egan, S. J.; Robson, R. *J. Am. Chem. Soc.* **1999**, *121*, 3535.

- (4) (a) Kuehl, C. J.; Kryschenko, Y. K.; Radhakrishnan, U.; Seidel, S. R.; Huang, S. D.; Stang, P. J. *Proc. Natl. Acad. Sci. U.S.A.* **2002**, *99*, 4932. (b) Kuehl, C. J.; Huang, S. D.; Stang, P. J. *J. Am. Chem. Soc.* **2001**, *123*, 9634. (c) Radhakrishnan, U.; Schweiger, M.; Stang, P. J. *Org. Lett.* **2001**, *3*, 3141. (d) Leninger, S.; Olenyuk, B.; Stang, P. J. *Chem. Rev.* **2000**, *100*, 853.
- (5) (a) Fujita, M.; Tominaga, M.; Hori, A.; Therrien, B. *Acc. Chem. Res.* **2005**, *38*, 371. (b) Tashiro, S.; Tominaga, M.; Kawano, M.; Therrien, B.; Ozeki, T.; Fujita, M. *J. Am. Chem. Soc.* **2005**, *127*, 4546. (c) Yoshizawa, M.; Tamura, M.; Fujita, M. *J. Am. Chem. Soc.* **2004**, *126*, 6846. (d) Yoshizawa, M.; Miyagi, S.; Kawano, M.; Ishiguro, K.; Fujita, M. *J. Am. Chem. Soc.* **2004**, *126*, 9172. (e) Kumazawa, K.; Biradha, K.; Kusakawa, T.; Okano, T.; Fujita, M. *Angew. Chem., Int. Ed.* **2003**, *42*, 3909. (f) Chand, D. K.; Biradha, K.; Fujita, M. *Chem. Commun.* **2001**, 1652.
- (6) (a) Argent, S. P.; Adams, H.; Riis-Johannessen, T.; Jeffery, J. C.; Harding, L. P.; Ward, M. H. D. *J. Am. Chem. Soc.* **2006**, *128*, 72. (b) Argent, S. P.; Adams, H.; Harding, L. P.; Ward, M. D. *Dalton Trans.* **2006**, 542.
- (7) (a) Yeh, R. M.; Xu, J.; Seeber, G.; Raymond, K. N. *Inorg. Chem.* **2005**, *44*, 6228. (b) Fiedler, D.; Pagliero, D.; Brumaghim, J. L.; Bergman, R. G.; Raymond, K. N. *Inorg. Chem.* **2004**, *43*, 846. (c) Caulder, D. L.; Brückner, C.; Powers, R. E.; König, S.; Parac, T. N.; Leary, J. A.; Raymond, K. N. *J. Am. Chem. Soc.* **2001**, *123*, 8923. (d) Caulder, D. L.; Raymond, K. N. *Acc. Chem. Res.* **1999**, *32*, 975.
- (8) (a) McMorran, D. A.; Steel, P. J. *Angew. Chem., Int. Ed.* **1998**, *37*, 3295. (b) Hartshorn, C. M.; Steel, P. J. *Chem. Commun.* **1997**, 541.

gomer metal arrays and polymeric metal chains.<sup>19</sup> This strategy is comparable to versatile methodologies<sup>20</sup> that either employ predesigned ligands, such as polypyridylamine ligands and  $\pi$ -conjugated linear polyenes, to position metal atoms in linear metal strings of  $M_n$  ( $n \geq 3$ ),<sup>21,22</sup> or use stable platinum blue ( $[\text{Pt}(\text{CN})_4]^{2-}$ ) and their rhodium or iridium derivatives as building blocks to construct linear backbones with metal–metal bonds.<sup>23</sup> In the course of our ongoing research on the design of metallocycles,<sup>11b,24</sup> we report herein the self-assembly of  $M_4L_2$ -type silver-based metalloprismatic coordination cages, which serve as building units for

subsequent assembly with  $\text{Ag}^+$  to afford an infinite chainlike supramolecular array with silver metal strings.

## Experimental Section

**Materials and General Methods.** Reagents were used as received without further purification.  $^1\text{H}$  NMR spectra were recorded on a Bruker AMX-400 FT-NMR spectrometer. Elemental analyses were performed by use of a Perkin-Elmer 2400 CHN elemental analyzer. Fast atom bombardment mass spectrometry (FAB-MS) data were obtained using a JMS-700 double-focusing mass spectrometer. Thermogravimetric (TG) analyses were performed under nitrogen with a Perkin-Elmer TGA-7 TG analyzer.

**Synthesis of 1,2,4,5-Tetrakis(benzoimidazol-1-ylmethyl)benzene (TBim).** KOH (1.10 g, 20.0 mmol) was slowly added to a solution of benzimidazole (1.57 g, 13.3 mmol) in tetrahydrofuran (THF; 50 mL) at room temperature with rigorous stirring. After approximately 4 h, a solution of 1,2,4,5-tetrakis(bromomethyl)benzene (1.50 g, 3.3 mmol) in 50 mL of THF was added dropwise, and the reaction mixture was stirred continuously overnight. The reaction solvent was subsequently removed under reduced pressure, and the residue was poured into 100 mL of water and extracted with dichloromethane ( $3 \times 50$  mL). The combined organic extracts were dried ( $\text{Na}_2\text{CO}_3$ ) and concentrated. The crude products were washed and purified using THF to afford white crystalline solids in 65% yield (1.30 g, 2.2 mmol).  $^1\text{H}$  NMR (400 MHz,  $\text{DMSO}-d_6$ ,  $\delta$ ): 8.16 (s, 4H,  $\text{H}^2$ ), 7.62 (d,  $J = 8.0$  Hz, 4H,  $\text{H}^4$ ), 7.16 (t,  $J = 7.2$  Hz, 4H,  $\text{H}^5$ ), 6.98 (d,  $J = 7.2$  Hz, 4H,  $\text{H}^6$ ), 6.93 (d,  $J = 8.0$  Hz, 4H,  $\text{H}^7$ ), 6.63 (s, 2H,  $\text{H}^{10}$ ), 5.53 (s, 8H,  $\text{H}^8$ ) ppm. FAB-MS ( $m/z$ ): 599  $[\text{M} + \text{H}]^+$ . Anal. Calcd for  $\text{C}_{38}\text{H}_{30}\text{N}_8 \cdot 1.5\text{H}_2\text{O}$ : C, 72.94; H, 5.32; N, 17.91. Found: C, 72.50; H, 5.54; N, 17.51.

**Synthesis of 1,2,4,5-Tetrakis(5,6-dimethylbenzimidazol-1-ylmethyl)benzene (TDMBim).** KOH (1.10 g, 20.0 mmol) was slowly added to a solution of 5,6-dimethylbenzimidazole (1.90 g, 13.3 mmol) in THF (50 mL) at room temperature with rigorous stirring. After approximately 4 h, a solution of 1,2,4,5-tetrakis(bromomethyl)benzene (1.50 g, 3.3 mmol) in 50 mL of THF was added dropwise, and the reaction mixture was stirred continuously overnight. The reaction solvent was subsequently removed under reduced pressure, and the residue was poured into 100 mL of water and extracted with dichloromethane ( $3 \times 50$  mL). The combined organic extracts were dried ( $\text{Na}_2\text{CO}_3$ ) and concentrated. The crude products were washed and purified using THF to afford white crystalline solids in 85% yield (2.00 g, 2.8 mmol).  $^1\text{H}$  NMR (400 MHz,  $\text{DMSO}-d_6$ ,  $\delta$ ): 8.03 (s, 4H,  $\text{H}^2$ ), 7.36 (s, 4H,  $\text{H}^4$ ), 6.75 (s, 4H,  $\text{H}^7$ ), 6.57 (s, 2H,  $\text{H}^{10}$ ), 5.43 (s, 8H,  $\text{H}^8$ ), 2.26 (s, 12H,  $\text{CH}_3$ ), 2.10 (s, 12H,  $\text{CH}_3$ ) ppm. FAB-MS ( $m/z$ ): 711  $[\text{M} + \text{H}]^+$ . Anal.

- (9) (a) Fan, J.; Zhu, H.-F.; Okamura, T.-a.; Sun, W.-Y.; Tang, W.-X.; Ueyama, N. *Chem.—Eur. J.* **2003**, *9*, 4724. (b) Fan, J.; Sun, W.-Y.; Okamura, T.-a.; Xie, J.; Tang, W.-X.; Ueyama, N. *New J. Chem.* **2002**, *26*, 199.
- (10) (a) Su, C.-Y.; Cai, Y.-P.; Chen, C.-L.; Smith, M. D.; Kaim, W.; zur Loye, H.-C. *J. Am. Chem. Soc.* **2003**, *125*, 8595. (b) Su, C.-Y.; Cai, Y.-P.; Chen, C.-L.; Lissner, F.; Kang, B.-S.; Kaim, W. *Angew. Chem., Int. Ed.* **2002**, *41*, 3371.
- (11) (a) Thanasekaran, P.; Liao, R.-T.; Liu, Y.-H.; Rajendran, T.; Rajagopal, S.; Lu, K.-L. *Coord. Chem. Rev.* **2005**, *249*, 1085. (b) Wu, H.-C.; Thanasekaran, P.; Tsai, C.-H.; Wu, J.-Y.; Huang, S.-M.; Wen, Y.-S.; Lu, K.-L. *Inorg. Chem.* **2006**, *45*, 295.
- (12) (a) Moon, D.; Kang, S.; Park, J.; Lee, K.; John, R. P.; Won, H.; Seong, G. H.; Kim, Y. S.; Kim, G. H.; Rhee, H.; Lah, M. S. *J. Am. Chem. Soc.* **2006**, *128*, 3530. (b) Owens, T. D.; Hollander, F. J.; Oliver, A. G.; Ellman, J. A. *J. Am. Chem. Soc.* **2001**, *123*, 1539.
- (13) (a) Zhang, J.; Miller, P. W.; Nieuwenhuyzen, M.; James, S. L. *Chem.—Eur. J.* **2006**, *12*, 2448. (b) Sumbly, C. J.; Hardie, M. J. *Angew. Chem., Int. Ed.* **2005**, *44*, 6395. (c) Müller, I. M.; Möller, D. *Angew. Chem., Int. Ed.* **2005**, *44*, 2969.
- (14) (a) Kim, D.; Paek, J. H.; Jun, M.-J.; Lee, J. Y.; Kang, S. O.; Ko, J. *Inorg. Chem.* **2005**, *44*, 7886. (b) Wu, B.; Yuan, D.; Lou, B.; Han, L.; Liu, C.; Zhang, C.; Hong, M. *Inorg. Chem.* **2005**, *44*, 9175.
- (15) (a) Sun, S.-S.; Stern, C. L.; Nguyen, S.-B. T.; Hupp, J. T. *J. Am. Chem. Soc.* **2004**, *126*, 6314. (b) Benkstein, K. D.; Hupp, J. T.; Stern, C. L. *Angew. Chem., Int. Ed.* **2000**, *39*, 2891.
- (16) (a) Rajendran, T.; Manimaran, B.; Liao, R.-T.; Lin, R.-J.; Thanasekaran, P.; Lee, G.-H.; Peng, S.-M.; Liu, Y.-H.; Chang, I.-J.; Rajagopal, S.; Lu, K.-L. *Inorg. Chem.* **2003**, *42*, 6388. (b) Rajendran, T.; Manimaran, B.; Lee, F.-Y.; Chen, P.-J.; Lin, S.-C.; Lee, G.-H.; Peng, S.-M.; Chen, Y.-J.; Lu, K.-L. *J. Chem. Soc., Dalton Trans.* **2001**, 3346.
- (17) For other recent examples, see: (a) Sun, S.-S.; Lees, A. J. *Chem. Commun.* **2001**, 103. (b) Sun, S.-S.; Lees, A. J. *J. Am. Chem. Soc.* **2000**, *122*, 8956. (c) Woessner, S. M.; Helms, J. B.; Shen, Y.; Sullivan, B. P. *Inorg. Chem.* **1998**, *37*, 5406.
- (18) (a) Steed, J. W.; Atwood, J. L. *Supramolecular Chemistry: a Concise Introduction*; John Wiley & Sons: Chichester, U.K., 2000. (b) Holliday, B. J.; Mirkin, C. A. *Angew. Chem., Int. Ed.* **2001**, *40*, 2022. (c) Parac, T. N.; Caulder, D. L.; Raymond, K. N. *J. Am. Chem. Soc.* **1998**, *120*, 8003. (d) Yue, N. L. S.; Jennings, M. C.; Puddephatt, R. J. *Inorg. Chem.* **2005**, *44*, 1125. (e) Dong, Y.-B.; Wang, P.; Ma, J.-P.; Zhao, X.-X.; Wang, H.-Y.; Tang, B.; Huang, R.-Q. *J. Am. Chem. Soc.* **2007**, *129*, 4872.
- (19) (a) Chen, J.-X.; Zhang, W.-H.; Tang, X.-Y.; Ren, Z.-G.; Li, H.-X.; Zhang, Y.; Lang, J.-P. *Inorg. Chem.* **2006**, *45*, 7671. (b) Patel, U.; Singh, H. B.; Wolmershäuser, G. *Angew. Chem., Int. Ed.* **2005**, *44*, 1715. (c) Yeh, T.-T.; Wu, J.-Y.; Wen, Y.-S.; Liu, Y.-H.; Twu, J.; Tao, Y.-T.; Lu, K.-L. *Dalton Trans.* **2005**, 656. (d) Hannon, M. J.; Painting, C. L.; Plummer, E. A.; Childs, L. J.; Alcock, N. W. *Chem.—Eur. J.* **2002**, *8*, 2225. (e) Yang, S.-P.; Chen, X.-M.; Ji, L.-N. *J. Chem. Soc., Dalton Trans.* **2000**, 2337.
- (20) Bera, J. K.; Dunbar, K. R. *Angew. Chem., Int. Ed.* **2002**, *41*, 4453.
- (21) (a) Berry, J. F.; Cotton, F. A.; Daniels, L. M.; Murillo, C. A. *J. Am. Chem. Soc.* **2002**, *124*, 3212. (b) Cotton, F. A.; Daniels, L. M.; Murillo, C. A.; Wang, X. *Chem. Commun.* **1999**, 2461. (c) Lai, S.-Y.; Lin, T.-W.; Chen, Y.-H.; Wang, C.-C.; Lee, G.-H.; Yang, M.-h.; Leung, M.-k.; Peng, S.-M. *J. Am. Chem. Soc.* **1999**, *121*, 250. (d) Tsao, T.-B.; Lee, G.-H.; Yeh, C.-Y.; Peng, S.-M. *Dalton Trans.* **2003**, 1465. (e) Rohmer, M.-M.; Strich, A.; Bénard, M.; Malrieu, J. P. *J. Am. Chem. Soc.* **2001**, *123*, 9126.
- (22) (a) Murahashi, T.; Nagai, T.; Mino, Y.; Mochizuki, E.; Kai, Y.; Kurosawa, H. *J. Am. Chem. Soc.* **2001**, *123*, 6927. (b) Murahashi, T.; Nagai, T.; Okuno, T.; Mastsutani, T.; Kurosawa, H. *Chem. Commun.* **2000**, 1689.
- (23) (a) Barton, J. K.; Rabinowitz, H. N.; Szalda, D. J.; Lippard, S. J. *J. Am. Chem. Soc.* **1977**, *99*, 2827. (b) Buss, C. E.; Mann, K. R. *J. Am. Chem. Soc.* **2002**, *124*, 1031. (c) Uemura, K.; Fukui, K.; Nishikawa, H.; Arai, S.; Matsumoto, K.; Oshio, H. *Angew. Chem., Int. Ed.* **2005**, *44*, 5459. (d) Mitsumi, M.; Golo, H.; Umebayashi, S.; Ozawa, Y.; Kobayashi, M.; Yokoyama, T.; Tanaka, H.; Kuroda, S.-i.; Toriumi, K. *Angew. Chem., Int. Ed.* **2005**, *44*, 4164. (e) Prater, M. E.; Pence, L. E.; Clérac, R.; Finniss, G. M.; Campana, C.; Auban-Senzier, P.; Jérôme, D.; Canadell, E.; Dunbar, K. R. *J. Am. Chem. Soc.* **1999**, *121*, 8005. (f) Tejel, C.; Ciriano, M. A.; Oro, L. A. *Chem.—Eur. J.* **1999**, *5*, 1131. (g) Tejel, C.; Ciriano, M. A.; Villarroja, B. E.; Gelpi, R.; López, J. A.; Lahoz, F. J.; Oro, L. A. *Angew. Chem., Int. Ed.* **2001**, *40*, 4084.
- (24) (a) Manimaran, B.; Thanasekaran, P.; Rajendran, T.; Lin, R.-J.; Chang, I.-J.; Lee, G.-H.; Peng, S.-M.; Rajagopal, S.; Lu, K.-L. *Inorg. Chem.* **2002**, *41*, 5323. (b) Manimaran, B.; Rajendran, T.; Lu, Y.-L.; Lee, G.-H.; Peng, S.-M.; Lu, K.-L. *J. Chem. Soc., Dalton Trans.* **2001**, 515. (c) Manimaran, B.; Thanasekaran, P.; Rajendran, T.; Liao, R.-T.; Liu, Y.-H.; Lee, G.-H.; Peng, S.-M.; Rajagopal, S.; Lu, K.-L. *Inorg. Chem.* **2003**, *42*, 4795. (d) Manimaran, B.; Rajendran, T.; Lu, Y.-L.; Lee, G.-H.; Peng, S.-M.; Lu, K.-L. *Eur. J. Inorg. Chem.* **2001**, 633.

Calcd for C<sub>46</sub>H<sub>46</sub>N<sub>8</sub>·H<sub>2</sub>O: C, 75.80; H, 6.64; N, 15.37. Found: C, 75.50; H, 6.12; N, 15.54.

**Self-Assembly of [Ag<sub>4</sub>(μ<sub>4</sub>-TBim)<sub>2</sub>(μ<sub>2</sub>-η<sup>2</sup>-NO<sub>3</sub>)<sub>2</sub>](NO<sub>3</sub>)<sub>2</sub>· $\frac{1}{2}$ CH<sub>2</sub>Cl<sub>2</sub>·2CH<sub>3</sub>OH (1· $\frac{1}{2}$ CH<sub>2</sub>Cl<sub>2</sub>·2CH<sub>3</sub>OH).** A solution of AgNO<sub>3</sub> (34.0 mg, 2.0 × 10<sup>-1</sup> mmol) in MeOH (5 mL) was carefully layered on top of a mixture of MeOH-CH<sub>2</sub>Cl<sub>2</sub> (10 mL, middle) and a solution of TBim (30.0 mg, 5.0 × 10<sup>-2</sup> mmol) in CH<sub>2</sub>Cl<sub>2</sub> (5 mL, bottom) at room temperature. The solution was allowed to stand for approximately 3 weeks, resulting in the formation of colorless crystals. Data for 1· $\frac{1}{2}$ CH<sub>2</sub>Cl<sub>2</sub>·2CH<sub>3</sub>OH. Yield: 44% (21.9 mg, 1.1 × 10<sup>-2</sup> mmol). <sup>1</sup>H NMR (400 MHz, DMF-*d*<sub>7</sub>, δ): 8.68 (s, 4H, H<sup>10</sup>), 8.09 (s, 8H, H<sup>2</sup>), 7.75 (d, *J* = 8.0 Hz, 8H, H<sup>4</sup>), 7.56 (d, *J* = 8.0 Hz, 8H, H<sup>7</sup>), 7.29–7.19 (m, 16H, H<sup>5</sup>, H<sup>6</sup>), 6.32 (d, *J* = 14.0 Hz, 8H, H<sup>8a</sup>), 5.68 (d, *J* = 14.0 Hz, 8H, H<sup>8b</sup>) ppm. FAB-MS (*m/z*): 1814 [Ag<sub>4</sub>(TBim)<sub>2</sub>(NO<sub>3</sub>)<sub>3</sub>]<sup>+</sup>. Anal. Calcd for C<sub>78.50</sub>H<sub>69</sub>Ag<sub>4</sub>ClN<sub>20</sub>O<sub>14</sub> (1· $\frac{1}{2}$ CH<sub>2</sub>Cl<sub>2</sub>·2CH<sub>3</sub>OH): C, 47.54; H, 3.51; N, 14.12. Found: C, 47.32; H, 3.52; N, 14.33.

**Self-Assembly of [(NO<sub>3</sub>)<sub>2</sub>][Ag<sub>4</sub>(μ<sub>4</sub>-TDMBim)<sub>2</sub>][Ag(NO<sub>3</sub>)<sub>2</sub>](NO<sub>3</sub>)<sub>2</sub>·CH<sub>2</sub>Cl<sub>2</sub>·CH<sub>3</sub>OH·4H<sub>2</sub>O (2·CH<sub>2</sub>Cl<sub>2</sub>·CH<sub>3</sub>OH·4H<sub>2</sub>O).** A solution of AgNO<sub>3</sub> (34.0 mg, 2.0 × 10<sup>-1</sup> mmol) in MeOH (5 mL) was carefully layered on top of a mixture of MeOH-CH<sub>2</sub>Cl<sub>2</sub> (10 mL, middle) and a solution of TDMBim (35.4 mg, 5.0 × 10<sup>-2</sup> mmol) in CH<sub>2</sub>Cl<sub>2</sub> (5 mL, bottom) at room temperature. The solution was allowed to stand for approximately 3 weeks, resulting in the formation of light-yellow crystals. Data for 2·CH<sub>2</sub>Cl<sub>2</sub>·CH<sub>3</sub>OH·4H<sub>2</sub>O. Yield: 8% (5.0 mg, 2.0 × 10<sup>-3</sup> mmol). <sup>1</sup>H NMR (400 MHz, DMSO-*d*<sub>6</sub>, δ): 8.39 (s, 4H, H<sup>10</sup>), 7.58 (br, 8H, H<sup>2</sup>), 7.42 (s, 8H, H<sup>4</sup>), 7.14 (s, 8H, H<sup>7</sup>), 6.02 (d, *J* = 13.4 Hz, 8H, H<sup>8a</sup>), 5.41 (d, *J* = 13.4 Hz, 8H, H<sup>8b</sup>), 2.32 (s, 24H, CH<sub>3</sub>), 2.30 (s, 24H, CH<sub>3</sub>) ppm. FAB-MS (*m/z*): 2039 [Ag<sub>4</sub>(TDMBim)<sub>2</sub>(NO<sub>3</sub>)<sub>3</sub>]<sup>+</sup>. Anal. Calcd for C<sub>93</sub>H<sub>104</sub>Ag<sub>5</sub>N<sub>21</sub>O<sub>20</sub> (2·CH<sub>3</sub>OH·4H<sub>2</sub>O): C, 47.03; H, 4.41; N, 12.38. Found: C, 47.35; H, 4.14; N, 12.32.

**Crystal Structure Determination.** Intensity data were collected at 273(2) K within the limits of 1.29° ≤ θ ≤ 25.03° and 1.14° ≤ θ ≤ 25.03° for 1· $\frac{1}{2}$ CH<sub>2</sub>Cl<sub>2</sub>·2CH<sub>3</sub>OH and 2·CH<sub>2</sub>Cl<sub>2</sub>·CH<sub>3</sub>OH·4H<sub>2</sub>O, respectively, using a Bruker Smart CCD diffractometer. The structures were solved with direct methods and refined by full-matrix least-squares methods on *F*<sup>2</sup> values using the WINGX<sup>25</sup> and SHELX-97<sup>26</sup> program packages. Anisotropic thermal factors were assigned to most of nonordered non-hydrogen atoms except those showing severe disorder as explained below. The positions of the C–H hydrogen atoms were generated geometrically and were assigned isotropic thermal parameters. In 2·CH<sub>2</sub>Cl<sub>2</sub>·CH<sub>3</sub>OH·4H<sub>2</sub>O, the metalloanion [Ag(NO<sub>3</sub>)<sub>2</sub>]<sup>-</sup> was found to be in disorder related to the symmetry of the structure and was, consequently, symmetrically modeled. One nitrate anion within the M<sub>4</sub>L<sub>2</sub> cage possesses a center of symmetry, *i*, located at the nitrogen atom (site occupation factor is 0.5). Two of the three oxygen atoms on the second nitrate counteranion, which is located at the general position, were disordered over four locations with refined site occupation factors of 0.68, 0.32, 0.54, and 0.46. One of the two water molecules was split over three positions with site occupancies of 0.44, 0.28, and 0.28. One CH<sub>3</sub>OH and one CH<sub>2</sub>Cl<sub>2</sub>, both with half-occupancy, were present in the asymmetric unit. Both chlorides on CH<sub>2</sub>Cl<sub>2</sub> were disordered with two occupied sites. The refined site occupation factors were 0.25/0.25 for one chloride atom and 0.28/0.22 for the second. Basic information pertaining to crystal parameters and structure refinement for 1· $\frac{1}{2}$ CH<sub>2</sub>Cl<sub>2</sub>·2CH<sub>3</sub>OH and

**Table 1.** Crystal Structure Refinement Data for 1· $\frac{1}{2}$ CH<sub>2</sub>Cl<sub>2</sub>·2CH<sub>3</sub>OH and 2·CH<sub>2</sub>Cl<sub>2</sub>·CH<sub>3</sub>OH·4H<sub>2</sub>O

|  | 1· $\frac{1}{2}$ CH <sub>2</sub> Cl <sub>2</sub> ·2CH <sub>3</sub> OH                | 2·CH <sub>2</sub> Cl <sub>2</sub> ·CH <sub>3</sub> OH·4H <sub>2</sub> O                          |
|--|--|--|
| formula  | C <sub>78.50</sub> H <sub>69</sub> Ag <sub>4</sub> ClN <sub>20</sub> O <sub>14</sub> | C <sub>94</sub> H <sub>106</sub> Ag <sub>5</sub> Cl <sub>2</sub> N <sub>21</sub> O <sub>20</sub> |
| fw   | 1983.47  | 2460.25  |
| cryst syst   | monoclinic   | triclinic  |
| space group  | <i>P</i> 2 <sub>1</sub> / <i>c</i>   | $\bar{P}1$   |
| <i>a</i> (Å)   | 15.7501(4)   | 8.2427(16)   |
| <i>b</i> (Å)   | 17.9067(5)   | 17.470(4)  |
| <i>c</i> (Å)   | 13.5423(4)   | 18.923(4)  |
| α (deg)  | 90   | 106.73(3)  |
| β (deg)  | 92.6120(10)  | 97.44(3)   |
| γ (deg)  | 90   | 97.77(3)   |
| <i>V</i> (Å <sup>3</sup> )                                     | 3815.40(18)  | 2544.6(9)  |
| <i>Z</i>   | 2  | 1  |
| λ (Å)  | 0.710 73   | 0.710 73   |
| <i>F</i> <sub>000</sub>  | 1994   | 1246   |
| ρ <sub>calcd</sub> (g cm <sup>-3</sup> )                       | 1.726  | 1.606  |
| μ (mm <sup>-1</sup> )  | 1.128  | 1.075  |
| GOF  | 1.049  | 1.066  |
| R1 <sup>w</sup> /wR2 <sup>b</sup> [ <i>I</i> > 2σ( <i>I</i> )] | 0.0478/0.1376  | 0.0508/0.1517  |
| R1 <sup>w</sup> /wR2 <sup>b</sup> (all data)                   | 0.0559/0.1448  | 0.0609/0.1608  |
| largest residuals (e Å <sup>-3</sup> )                         | 2.397/−3.672   | 1.585/−1.643   |

<sup>a</sup> R1 = Σ|*F*<sub>o</sub> − |*F*|Σ|*F*<sub>o</sub>|. <sup>b</sup> wR2 = {Σ[*w*(*F*<sub>o</sub><sup>2</sup> − *F*<sub>c</sub><sup>2</sup>)]/Σ[*w*(*F*<sub>o</sub><sup>2</sup>)]<sup>1/2</sup>.

**Table 2.** Selected Bond Lengths [Å] and Angles [deg] for 1· $\frac{1}{2}$ CH<sub>2</sub>Cl<sub>2</sub>·2CH<sub>3</sub>OH and 2·CH<sub>2</sub>Cl<sub>2</sub>·CH<sub>3</sub>OH·4H<sub>2</sub>O<sup>a</sup>

| 1· $\frac{1}{2}$ CH <sub>2</sub> Cl <sub>2</sub> ·2CH <sub>3</sub> OH   |            |               |            |
|---|------------|---------------|------------|
| Ag1–N1  | 2.107(4)   | Ag1–N5        | 2.111(4)   |
| Ag1–O11   | 2.550(4)   | Ag2–N3        | 2.107(5)   |
| Ag2–N7  | 2.112(4)   | Ag2–O12       | 2.582(4)   |
| N1–Ag1–N5   | 167.66(17) | N1–Ag1–O11    | 102.31(16) |
| N5–Ag1–O11  | 89.87(15)  | N3–Ag2–N7     | 168.43(18) |
| N3–Ag2–O12  | 100.61(16) | N7–Ag2–O12    | 90.72(16)  |
| 2·CH <sub>2</sub> Cl <sub>2</sub> ·CH <sub>3</sub> OH·4H <sub>2</sub> O |            |               |            |
| Ag1–N3  | 2.103(4)   | Ag1–N1        | 2.107(4)   |
| Ag1–O13#1   | 2.513(9)   | Ag1–O11       | 2.575(8)   |
| Ag2–N5  | 2.110(4)   | Ag2–N7        | 2.113(5)   |
| Ag3–O21   | 2.139(5)   | Ag3–O22#2     | 2.225(4)   |
| Ag3–O22   | 2.583(4)   |               |            |
| N3–Ag1–N1   | 160.70(17) | N3–Ag1–O13#1  | 107.9(4)   |
| N1–Ag1–O13#1  | 90.6(3)    | N3–Ag1–O11    | 82.4(2)    |
| N1–Ag1–O11  | 116.1(2)   | O13#1–Ag1–O11 | 25.5(3)    |
| N5–Ag2–N7   | 164.76(17) | O21–Ag3–O22#2 | 153.13(16) |
| O21–Ag3–O22   | 53.27(14)  | O22#2–Ag3–O22 | 153.51(7)  |

<sup>a</sup> Symmetry operations for 2·CH<sub>2</sub>Cl<sub>2</sub>·CH<sub>3</sub>OH·4H<sub>2</sub>O: #1, −*x* + 1, −*y* + 1, −*z* + 1; #2, −*x*, −*y* + 1, −*z* + 1.

2·CH<sub>2</sub>Cl<sub>2</sub>·CH<sub>3</sub>OH·4H<sub>2</sub>O is summarized in Table 1, and selected bond lengths and angles are provided in Table 2.

## Results and Discussion

**Design and Synthesis of the Tetratopic Ligands TBim and TDMBim.** Semirigid ligands have flexible freely rotating arms and allow diverse conformations. As a consequence, they are excellent candidates for the synthesis of extended coordination structures<sup>27–30</sup> and discrete M<sub>4</sub>L<sub>2</sub>-type

(25) Farrugia, L. J. *J. Appl. Crystallogr.* **1999**, *32*, 837.

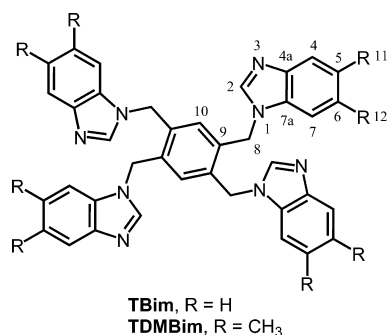
(26) Sheldrick, G. M. *SHELX-97 (including SHELXS and SHELXL)*, A Program for Crystal Structure Solution and Refinement; University of Göttingen: Göttingen, Germany, 1997.

(27) (a) Carlucci, L.; Ciani, G.; Proserpio, D. M. *Cryst. Growth Des.* **2005**, *5*, 37. (b) Carlucci, L.; Ciani, G.; Proserpio, D. M. *Chem. Commun.* **2004**, 380.

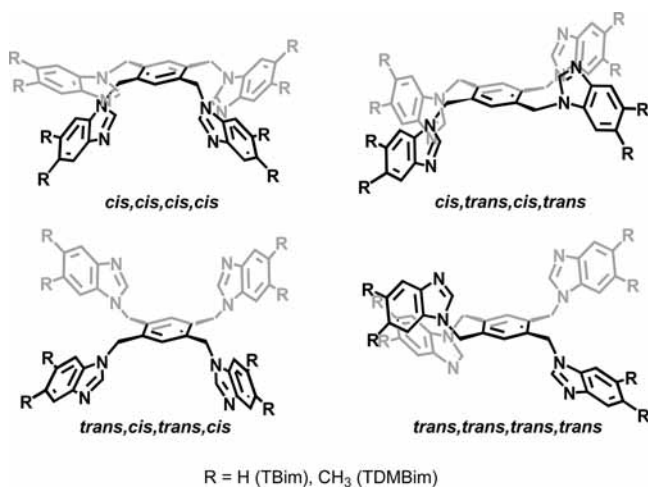
(28) (a) Lu, X.-Q.; Jiang, J.-J.; zur Loye, H.-C.; Kang, B.-S.; Su, C.-Y. *Inorg. Chem.* **2005**, *44*, 1810. (b) Su, C.-Y.; Smith, M. D.; zur Loye, H.-C. *Angew. Chem., Int. Ed.* **2003**, *42*, 4085.

(29) (a) Fan, J.; Sun, W.-Y.; Okamura, Y.-a.; Zheng, Y.-Q.; Sui, B.; Tang, W.-X.; Ueyama, N. *Cryst. Growth Des.* **2004**, *4*, 579. (b) Fan, J.; Sun, W.-Y.; Okamura, T.-a.; Tang, W.-X.; Ueyama, N. *Inorg. Chem.* **2003**, *42*, 3168. (c) Fan, J.; Zhu, H.-F.; Okamura, T.-a.; Sun, W.-Y.; Tang, W.-X.; Ueyama, N. *Inorg. Chem.* **2003**, *42*, 158. (d) Fan, J.; Sui, B.; Okamura, T.-a.; Sun, W.-Y.; Tang, W.-X.; Ueyama, N. *J. Chem. Soc., Dalton Trans.* **2002**, 3868.

Scheme 1



Scheme 2. Possible Structural Conformations of the Semirigid Tetratopic Ligands TBim and TDMBim

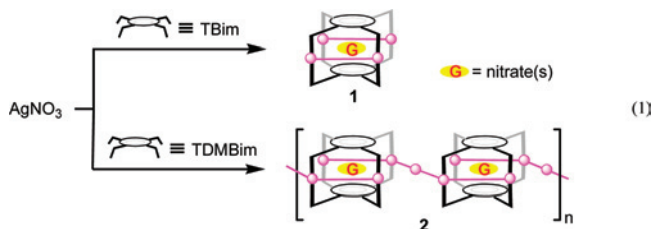


molecules with variable values of  $x$  and  $y$ .<sup>8–10</sup> To design ligands suitable for the assembly of new molecular structures, two semirigid tetratopic ligands, TBim and TDMBim (Scheme 1), were synthesized in high yields from the reaction of 1,2,4,5-tetrakis(bromomethyl)benzene with benzimidazole or 5,6-dimethylbenzimidazole, respectively, under strong alkaline (KOH) conditions. Ligand structures were characterized by NMR, MS, and elemental analysis. The methyl substituents on the 5 and 6 positions of the benzimidazole group in TDMBim increase the solubility and yield of the tetratopic ligand. To our knowledge, this type of tetratopic ligand (TBim and TDMBim) is designed and synthesized for the first time, although a number of semirigid ditopic and tritopic ligands have been published.<sup>8–10,27–30</sup>

**Self-Assembled Synthesis and Characterization of Ag<sub>4</sub>L<sub>2</sub> Cages.** The formation of discrete hollow structures is controlled by the stereochemical preferences of the metal ion and the nature of the ligands, including the donor sets, the number and position of coordinating groups, as well as the flexibility or rigidity of the linker groups joining the coordination sites.<sup>31</sup> Silver(I) is well suited for the design of complex supramolecular materials because of its various

stereochemical and geometric configurations, as well as coordination numbers ranging from 2 to 6.<sup>32</sup> The predesigned tetratopic semirigid ligands, TBim and TDMBim, exhibit several geometries, such as cis,cis,cis,cis, cis,trans,cis,trans, trans,cis,trans,cis, and trans,trans,trans,trans conformations and so on (Scheme 2), because of the rotating arms with nitrogen-donor Bim coordination (Bim = benzimidazole) connected by methylene groups. Both ligands are expected to facilitate prismatic cage-structure formation if the four Bim arms take the bowl-shaped cis,cis,cis,cis conformation.

Colorless crystals of [Ag<sub>4</sub>(μ<sub>4</sub>-TBim)<sub>2</sub>(μ<sub>2</sub>-η<sup>2</sup>-NO<sub>3</sub>)<sub>2</sub>](NO<sub>3</sub>)<sub>2</sub> · 1/2CH<sub>2</sub>Cl<sub>2</sub> · 2CH<sub>3</sub>OH (**1** · 1/2CH<sub>2</sub>Cl<sub>2</sub> · 2CH<sub>3</sub>OH) and light-yellow crystals of [(NO<sub>3</sub>)<sup>-</sup>C{Ag<sub>4</sub>(μ<sub>4</sub>-TDMBim)<sub>2</sub>}] [Ag(NO<sub>3</sub>)<sub>2</sub>](NO<sub>3</sub>)<sub>2</sub> · CH<sub>2</sub>Cl<sub>2</sub> · CH<sub>3</sub>OH · 4H<sub>2</sub>O (**2** · CH<sub>2</sub>Cl<sub>2</sub> · CH<sub>3</sub>OH · 4H<sub>2</sub>O) were obtained from the self-assembly of AgNO<sub>3</sub> with TBim or TDMBim, respectively, at ambient temperature (eq 1).



Characterization of the solution structures of **1** and **2** was performed by dissolving crystalline samples in DMF-*d*<sub>7</sub> and DMSO-*d*<sub>6</sub>, respectively. <sup>1</sup>H NMR spectra of the ligand, TDMBim, and complex **2** showed that the proton, H<sup>2</sup>, is shifted upfield, while H<sup>4</sup>, H<sup>7</sup>, H<sup>8</sup>, and H<sup>10</sup> are shifted downfield upon coordination of the ligand (see parts a and e of Figure 7). It is well-known that the downfield chemical shifts of the ligand protons occur as a result of a loss in electron density upon coordination to metal ions.<sup>4a,b</sup> In the present study, H<sup>10</sup>, which was shifted downfield by 1.82 ppm, exhibited the most marked change. In contrast, the tiny upfield shift ( $\Delta\delta = 0.45$  ppm) observed for H<sup>2</sup> agrees with the formation of a prismatic cage structure [Ag<sub>4</sub>(μ<sub>4</sub>-TDMBim)<sub>2</sub>]<sup>4+</sup> in solution. The vertical head-to-head syn conformation of the ligand TDMBim allows the ring current from the arene core to shield H<sup>2</sup>. Also of interest is the observation that signals for H<sup>8</sup> protons were divided into two sets of doublets with identical integral values but different chemical shifts. This result suggests the assembly of metalloprismatic cage structures in solution, allowing two types of H<sup>8</sup> protons (H<sup>8a</sup> and H<sup>8b</sup>) present in different magnetic (chemical) environments: one is deshielded (greater downfield shift) by the ring current effect of the two parallel Bim moieties in the cage structure, while the other H<sup>8</sup> proton is not. Convincing support for the solution structure was provided by FAB-MS, the results of which were dominated by a peak corresponding to [Ag<sub>4</sub>(TDMBim)<sub>2</sub>(NO<sub>3</sub>)<sub>3</sub>]<sup>+</sup> ( $m/z = 2039$ ; Figure S8 in the Supporting Information). TBim and the silver(I) complex **1** exhibited similar changes in chemical shifts and MS results (Figures S5 and S6 in the Supporting Information), supporting a tetragonal metallocage solution structure of **1**.

**Solid-State Structure Description.** Solid-state structures of **1** and **2** were determined by single-crystal X-ray diffrac-

(30) (a) Zhang, L.; Lü, X.-Q.; Chen, C.-L.; Tan, H.-Y.; Zhang, H.-X.; Kang, B.-S. *Cryst. Growth Des.* **2005**, *5*, 283. (b) Ohi, H.; Tachi, Y.; Itoh, S. *Inorg. Chem.* **2004**, *43*, 4561. (c) Raehm, L.; Mimassi, L.; Guyard-Duhayon, C.; Amouri, H.; Rager, M. N. *Inorg. Chem.* **2003**, *42*, 5654. (31) Reger, D. L.; Semeniuc, R. F.; Rassolov, V.; Smith, M. D. *Inorg. Chem.* **2004**, *43*, 537, and references cited therein.

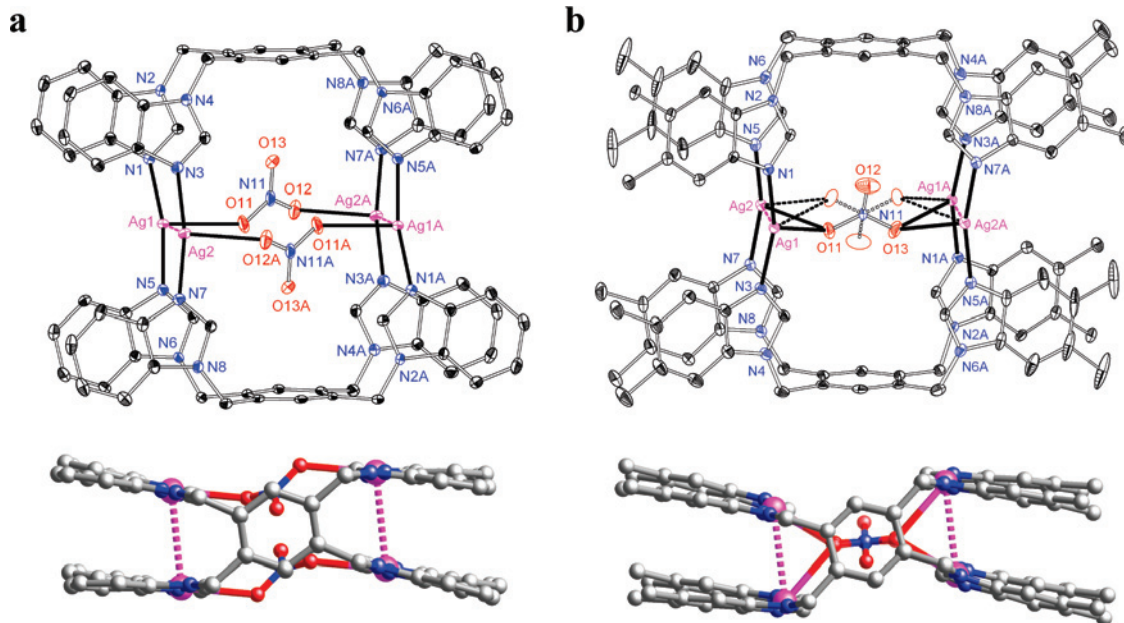


**Figure 1.** Side view (upper) and top view (lower) of the  $[\text{Ag}_4(\mu_4\text{-TBim})_2(\mu_2\text{-}\eta^2\text{-NO}_3)_2]^{2+}$  cage with a  $\text{Ag1}\cdots\text{Ag2}$  distance of 3.3231(6) Å in  $1 \cdot \frac{1}{2}\text{CH}_2\text{Cl}_2 \cdot 2\text{CH}_3\text{OH}$  (a) and the  $[(\text{NO}_3)^-\text{C}\{\text{Ag}_4(\mu_4\text{-TDMBim})_2\}]^{3+}$  cage with a  $\text{Ag1}\cdots\text{Ag2}$  distance of 3.3059(10) Å in  $2 \cdot \text{CH}_2\text{Cl}_2 \cdot \text{CH}_3\text{OH} \cdot 4\text{H}_2\text{O}$  (b).

tion analysis. Both compounds adopt a  $\text{M}_4\text{L}_2$ -type tetragonal metalloprismatic cage structure,  $[\text{Ag}_4(\mu_4\text{-L})_2]^{4+}$  (**1**,  $\text{L} = \text{TBim}$ ; **2**,  $\text{L} = \text{TDMBim}$ ), produced by two face-to-face-positioned TBim or TDMBim ligands in *cis,cis,cis,cis* conformation and four two-coordinated silver(I) ions, with heights of 10.85 Å for **1** and 11.13 Å for **2** (Figure 1). Intramolecular  $\text{Ag}\cdots\text{Ag}$  contacts [3.3231(6) Å for **1** and 3.3059(10) Å for **2**] and weak  $\pi\text{-}\pi$  interactions between parallel benzimidazolyl rings at the ortho positions of the benzene ring (average  $\text{C}\cdots\text{C}$  distances are 3.50 and 3.53 Å for **1** and 3.54 and 3.56 Å for **2**; dihedral angles are 7.96 and 9.18° for **1** and 6.63 and 8.01° for **2**) stabilized the molecular structures.

Although **1** and **2** have similar cationic  $\text{M}_4\text{L}_2$  cage structures, they exhibit significantly different nitrate-anion-trapping characteristics. In **1**, two nitrate anions are located at the two large windows of the tetragonal metalloprismatic cage and each of them is coordinated to two silver atoms [ $\text{Ag}\text{-O}$  2.550(4)–2.582(4) Å] with an anti,anti- $\mu_2\text{-}\eta^2$ -bonding mode. Notably, the oxygen (O13) atom that remains free is perpendicular to the center of the arene core of the TBim ligand at a distance of 3.41 Å, as shown in Figure 2. This geometry suggests possible  $\text{O}\cdots\pi$  (anion- $\pi$ ) interactions, which are extremely rare.<sup>33</sup> The oxygen atom also interacts with the Bim hydrogen ( $\text{H}^2$ ) atoms of the TBim ligand via  $\text{C}\text{-H}\cdots\text{O}$  interactions ( $\text{C}\cdots\text{O}$  3.20–3.48 Å;  $\text{C}\text{-H}\cdots\text{O}$  137–166°). Each  $[\text{Ag}_4(\mu_4\text{-TBim})_2(\mu_2\text{-}\eta^2\text{-NO}_3)_2]^{2+}$  cage interacts with two cocrystallized methanol molecules via coordinated nitrate oxygen atoms through bifurcated  $\text{O}\text{-H}\cdots\text{O}$  hydrogen-bonding interactions ( $\text{O}\cdots\text{O}$  3.01–3.05 Å;  $\text{O}\text{-H}\cdots\text{O}$  149–151°) to form a hydrogen-bonded 1:2 cage/solvent

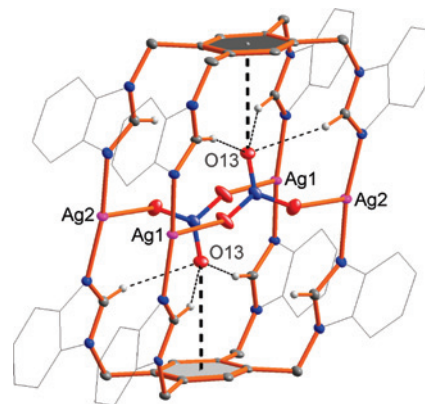


**Figure 2.** Representation of possible  $\text{O}\cdots\pi$  interactions (bold dashed lines) between the nitrate oxygen atom that remains free and the central arene core of the TBim ligand and  $\text{C}\text{-H}\cdots\text{O}$  interactions (thin dashed lines) between the same nitrate oxygen atom and the Bim hydrogen atoms of the TBim ligand in **1**.

complex, which is stacked along the *c* axis via alternate intra- and intermolecular  $\pi\text{-}\pi$  stacking interactions (Figure 3).

The crystal structure of **2** is of particular interest. As shown in Figure 4, the disordered  $\text{Ag}^+$  ions act as linkers connecting two adjacent charged cages  $[(\text{NO}_3)^-\text{C}\{\text{Ag}_4(\mu_4\text{-TDMBim})_2\}]^{3+}$  into a one-dimensional supramolecular array via ligand-unsupported argentophilicity [ $\text{Ag}\cdots\text{Ag}$  3.2375(17)–3.2759(18) Å]. These cage-chain arrays pack in a gridlike manner, in which the large interchain voids accommodated free nitrate anions and lattice solvent ( $\text{CH}_2\text{Cl}_2$ ,  $\text{CH}_3\text{OH}$ , and  $\text{H}_2\text{O}$ ) molecules (Figure 5). A few compounds, either aggregated by strong metal-donor coordination bonds<sup>10a,34</sup> or connected by weak noncovalent interactions, such as

(32) Suenga, Y.; Kuroda-Sowa, T.; Maekawa, M.; Munakata, M. *J. Chem. Soc., Dalton Trans.* **2000**, 3620, and references cited therein.

(33) (a) Egli, M.; Sarkhel, S. *Acc. Chem. Res.* **2007**, *40*, 197. (b) Zhou, X.-P.; Zhang, X.; Lin, S.-H.; Li, D. *Cryst. Growth Des.* **2007**, *7*, 485. (c) Gural'skiy, I. A.; Solntsev, P. V.; Krautscheidb, H.; Domasevitch, K. V. *Chem. Commun.* **2006**, 4808. (d) Yoshizawa, M.; Kusukawa, T.; Kawano, M.; Ohhara, T.; Tanaka, I.; Kurihara, K.; Niimura, N.; Fujita, M. *J. Am. Chem. Soc.* **2005**, *127*, 2798.

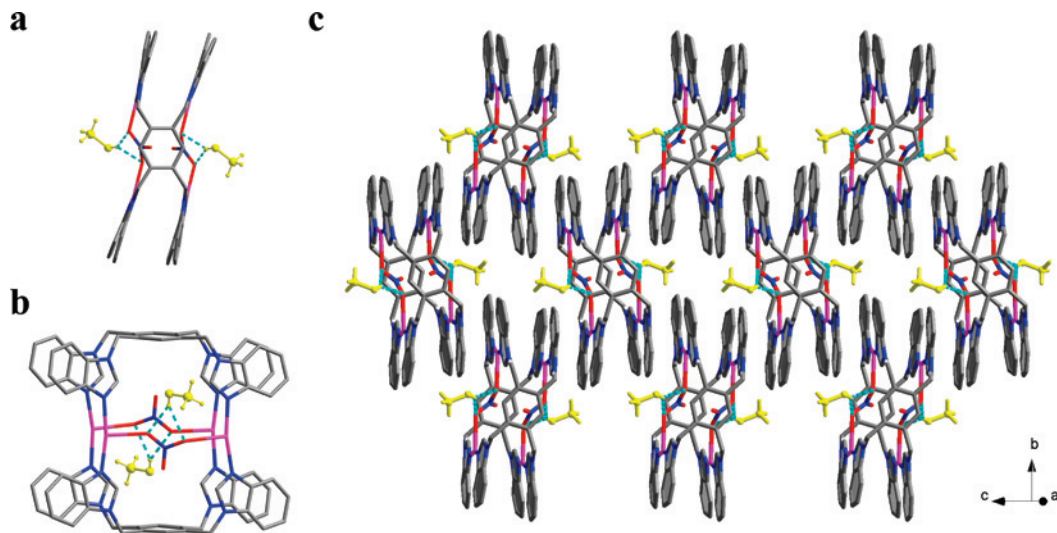


**Figure 3.** (a) Top and (b) side views of the hydrogen-bonded 1:2 cage/solvent complex in  $1 \cdot \frac{1}{2}\text{CH}_2\text{Cl}_2 \cdot 2\text{CH}_3\text{OH}$ . (c) Representation of the packing diagram of  $1 \cdot \frac{1}{2}\text{CH}_2\text{Cl}_2 \cdot 2\text{CH}_3\text{OH}$ , showing alternate intra- and intermolecular  $\pi$ - $\pi$  stacking interactions along the  $c$  axis. Charge-complemented free nitrate anions and cocrystallized dichloromethane molecules are omitted for clarity. Color code: Ag, pink; O, red; N, blue; C, gray; H, white; methanol molecules, yellow; O-H...O hydrogen bonds, cyan dashed lines.

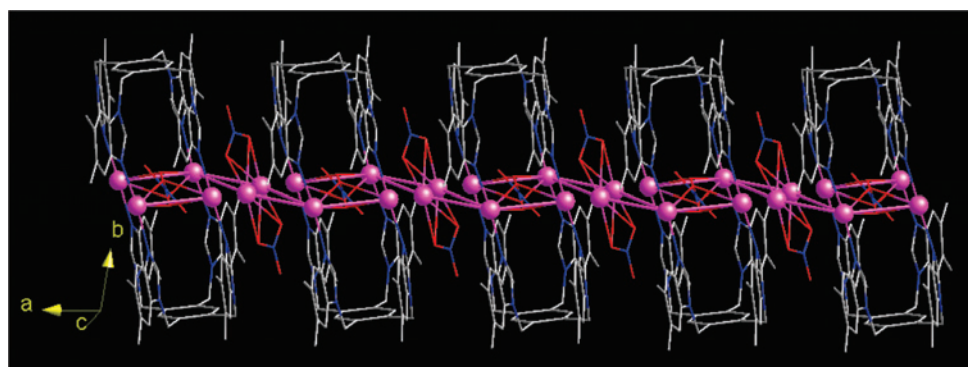


**Figure 4.** Perspective view of a supramolecular array of cages with silver metal strings, constructed by alternating cationic  $\text{M}_4\text{L}_2$ -type cages,  $[(\text{NO}_3^-)_2\text{C}\{\text{Ag}_4(\mu_4\text{-TDMBim})_2\}]^{3+}$ , and  $\text{Ag}^+$  linkages in  $2 \cdot \text{CH}_2\text{Cl}_2 \cdot \text{CH}_3\text{OH} \cdot 4\text{H}_2\text{O}$ . The  $\text{Ag} \cdots \text{Ag}$  distances range from 3.2375(17) to 3.3059(10) Å.

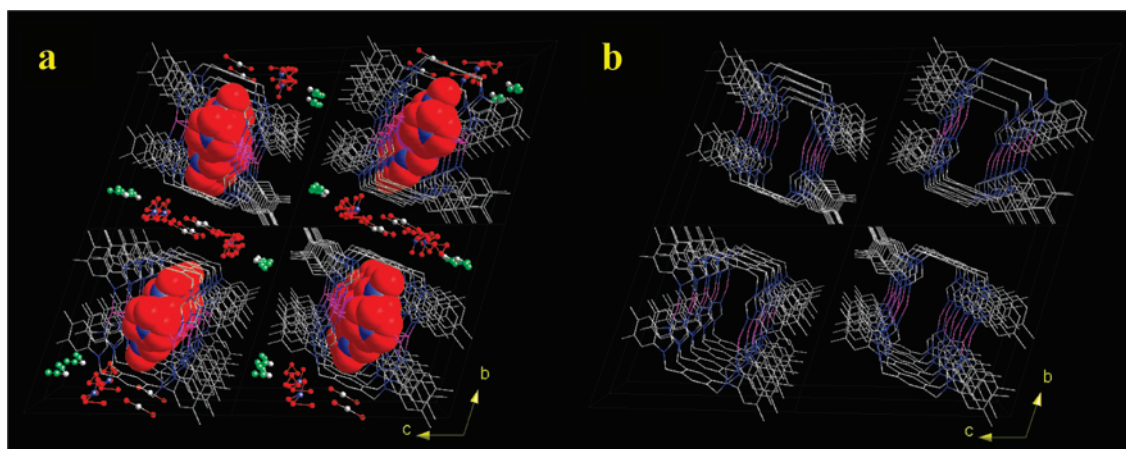


**Figure 5.** Representation of the packing diagram of  $2 \cdot \text{CH}_2\text{Cl}_2 \cdot \text{CH}_3\text{OH} \cdot 4\text{H}_2\text{O}$  in a gridlike manner, showing one-dimensional channels within the cage chain and large interchain voids with (a) and without (b)  $[\text{Ag}(\text{NO}_3)_2]^-$  linkers, guest and uncoordinated nitrate anions, and solvent molecules. Color code: pink, Ag; red, O; blue, N; gray, C; green, Cl.

hydrogen bonds<sup>9a</sup> and  $\pi$ - $\pi$  contacts,<sup>35</sup> have been reported. However, to the best of our knowledge, infinite one-dimensional arrangements of cage molecules formed by

metal-metal attractions, as shown in **2**, are reported herein for the first time. It is noteworthy that every five silver atoms from two adjacent cages and one disordered  $\text{Ag}^+$  linker in the cage chain form a resonant silver string with an overall length of 12.17 Å via silver-silver interactions, providing new insight into the formation of metal strings. In **2**, there

(34) (a) Cheng, A.-L.; Liu, N.; Zhang, J.-Y.; Gao, E.-Q. *Inorg. Chem.* **2007**, *46*, 1034. (b) Hannon, M. J.; Painting, C. L.; Errington, W. *Chem. Commun.* **1997**, 1805.

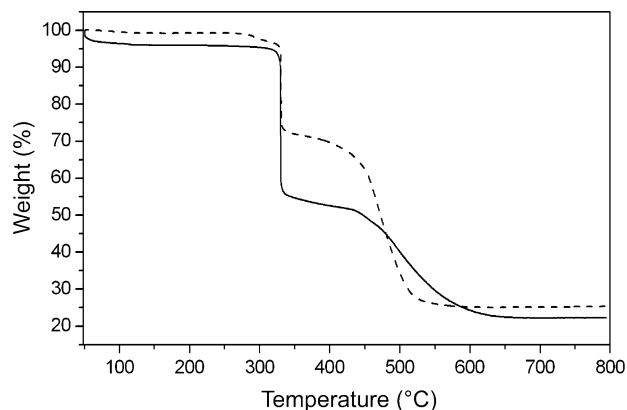


**Figure 6.** TG curves of  $1 \cdot \frac{1}{2} \text{CH}_2\text{Cl}_2 \cdot 2 \text{CH}_3\text{OH}$  (solid line) and  $2 \cdot \text{CH}_3\text{OH} \cdot 4 \text{H}_2\text{O}$  (dashed line).

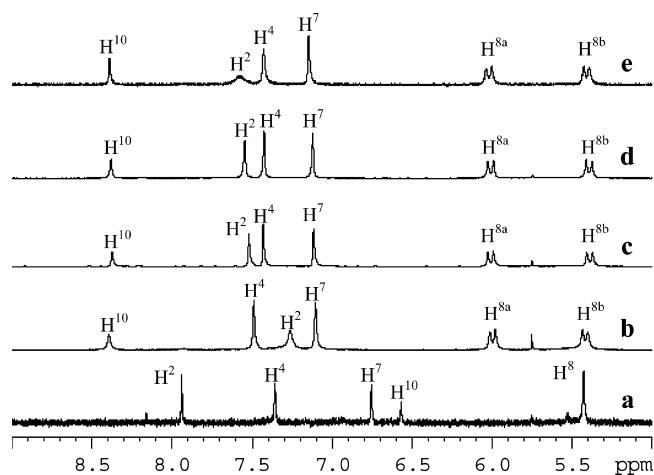


**Figure 7.** Partial  $^1\text{H}$  NMR spectra of (a) the ligand TDMBim, (b) the reaction mixture with an M:L = 2:2 ratio, (c) the reaction mixture with an M:L = 4:2 ratio, (d) the reaction mixture with an M:L = 5:2 ratio, and (e) the silver(I) complex **2** in  $\text{DMSO}-d_6$ . The atomic numbering scheme for protons is the same as that for the carbon atoms in Scheme 1.

is only one disordered nitrate anion encapsulated by the cage, which is comparable to that in **1**. The  $\text{Ag}^+$  linkage outside the cage is further coordinated by two chelated nitrate groups to give a metalloanion  $[\text{Ag}(\text{NO}_3)_2]^-$ , which is in disorder relative to the symmetry of the structure and is, consequently, symmetrically modeled. To the best of our knowledge,  $[\text{Ag}_x(\text{NO}_3)_y]^{(y-x)-}$ -type metalloanions are less common.<sup>9a,36</sup>

**Thermal Stability of Ag<sub>4</sub>L<sub>2</sub> Cages.** TG analyses of  $1 \cdot \frac{1}{2} \text{CH}_2\text{Cl}_2 \cdot 2 \text{CH}_3\text{OH}$  and  $2 \cdot \text{CH}_3\text{OH} \cdot 4 \text{H}_2\text{O}$  were performed on polycrystalline samples under a nitrogen atmosphere in studying their thermal stabilities. The results of TG analyses, which were in agreement with those from the microanalyses, indicate that Ag<sub>4</sub>L<sub>2</sub> cages **1** and **2** both are thermally stable up to 330 °C (Figure 6). The TG curves of both samples reveal that the release of lattice solvent molecules, i.e.,  $\text{CH}_2\text{Cl}_2$  and  $\text{CH}_3\text{OH}$  in  $1 \cdot \frac{1}{2} \text{CH}_2\text{Cl}_2 \cdot 2 \text{CH}_3\text{OH}$  (found 5.1%; calcd 5.4%) and  $\text{CH}_3\text{OH}$  and  $\text{H}_2\text{O}$  in  $2 \cdot \text{CH}_3\text{OH} \cdot 4 \text{H}_2\text{O}$  (found 3.8%; calcd 4.4%), occurred from room temperature to 330 °C, following a decomposition process to give a final residual of Ag<sub>2</sub>O composition (for  $1 \cdot \frac{1}{2} \text{CH}_2\text{Cl}_2 \cdot 2 \text{CH}_3\text{OH}$ , found

22.5% at 650 °C, calcd 23.4%; for  $2 \cdot \text{CH}_3\text{OH} \cdot 4 \text{H}_2\text{O}$ , found 25.5% at 575 °C, calcd 24.4%).

**Dynamics Studies.** To understand the details of self-organization of silver(I) complexes **1** and **2**, an in situ  $^1\text{H}$  NMR study was performed at room temperature. Figure 7 depicts the partial  $^1\text{H}$  NMR spectra for in situ spectral monitoring of reactions between TDMBim and  $\text{AgNO}_3$  with different metal-to-ligand ratios in  $\text{DMSO}-d_6$  at room temperature.

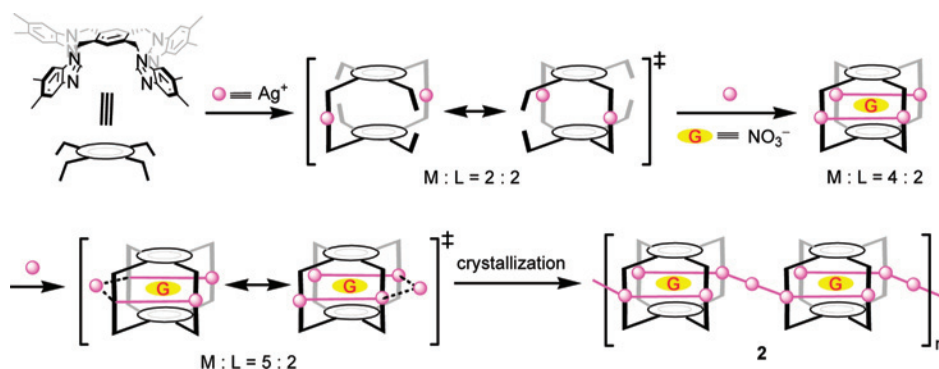
When the reaction was performed using an M:L = 2:2 ratio (Figure 7b), in situ  $^1\text{H}$  NMR indicates that all proton signals were shifted (downfield or upfield) but no “free” TDMBim signals were evident. These results clearly demonstrate metal complexation in solution. The relatively broad patterns also suggest that, although the cage structure is formed in solution, the silver(I) ions are not saturated and are rapidly exchanged among the four coordination sites of the TDMBim ligand, leading to dynamic equilibrium on the NMR time scale. All proton signals were similar to that of **2**, except the proton H<sup>2</sup> signal, which is shifted upfield by 0.77 ppm and is comparable to that of “free” TDMBim (Figure 7e). The  $^1\text{H}$  NMR spectrum of the reaction mixture with a metal-to-ligand ratio of 4:2 shows that the H<sup>2</sup> proton is shifted downfield, while other proton signals remain nearly unchanged (Figure 7c). This result may be explained by encapsulation of nitrate groups. The addition of excess metal salt leads to further downfield shifts in the H<sup>2</sup> proton (Figure 7d). This phenomenon is most likely attributed to the influence of cage...Ag<sup>+</sup> contacts,<sup>37</sup> in spite of the fact that the interaction between the metallocycles and silver ions is considerably very weak in solution and the further downfield shift of the H<sup>2</sup> proton in the  $^1\text{H}$  NMR spectrum is very small. In addition, the H<sup>8</sup> protons for all metal-to-ligand ratios always divide into two different chemical shifts with identical doublet integral values, indicating complexation of the single species, i.e., the metalloprismatic cage structure, in solution. Moreover, variable-temperature  $^1\text{H}$  NMR studies also revealed that the proton signals of TDMBim in **2** do not show significant shifts as the temperature was increased from 308 to 359 K, implying that the cage structure of **2** in solution is preserved upon heating. These results suggest that the reaction is thermodynamically controlled and that the present molecular structures are both kinetically and thermodynamically stable.<sup>10a</sup> In the present system, in situ  $^1\text{H}$  NMR results for the generation of **2** provide strong evidence for the hypothesis that the M<sub>4</sub>L<sub>2</sub>-type cage structure initially forms in solution, followed by connection of  $[\text{Ag}(\text{NO}_3)_2]^-$  metalloanions to form the final chainlike structure as shown in Scheme 3.

A comparison of  $^1\text{H}$  NMR chemical shifts for different protons may identify the dominant coordination mode in solution, especially when used in conjunction with the solid-state structural pattern.<sup>10a</sup> These methods are valid even though silver(I) complexes are normally labile and rapid

(35) Hu, T.-L.; Li, J.-R.; Xie, Y.-B.; Bu, X.-H. *Cryst. Growth Des.* **2006**, *6*, 648.

(36) Neumüller, B.; Weller, F.; Schmock, F.; Dehnicke, K. *Z. Anorg. Allg. Chem.* **2005**, *631*, 1767.

(37) Manimaran, B.; Lai, L.-J.; Thanasekaran, P.; Wu, J.-Y.; Liao, R.-T.; Tseng, T.-W.; Liu, Y.-H.; Lee, G.-H.; Peng, S.-M.; Lu, K.-L. *Inorg. Chem.* **2006**, *45*, 8070.

**Scheme 3.** Schematic Representation of a Potential Mechanism for the Formation of a Chainlike Supramolecular Array of  $\text{Ag}_4\text{L}_2$  Cages

chemical exchange may occur on the NMR time scale at room temperature.<sup>38</sup>

### Conclusions

In this study, nanoscale chainlike supramolecular arrays could be ordered through nanocages as secondary building blocks. The semirigid tetrapotic ligands TBim and TDMBim take on a bowl-shaped cis,cis,cis,cis conformation, leading to the formation of **1** and **2**, respectively. Both compounds adopt a  $M_4L_2$ -type tetragonal metalloprismatic cage structure,  $[\text{Ag}_4(\mu_4\text{-L})_2]^{4+}$ , with strong intramolecular silver–silver contacts. Complex **1** is a discrete species, while complex **2** is a novel infinite chainlike supramolecular array involving silver metal strings assembled from  $[\text{Ag}_4(\mu_4\text{-L})_2]^{4+}$  nanocages

and silver linkages. Results of an in situ  $^1\text{H}$  NMR study unambiguously revealed the successive self-organization process, in which self-organization of the molecular cage takes place initially, followed by crystallization of the corresponding supramolecular arrays with silver metal strings.

**Acknowledgment.** We are grateful to Academia Sinica and the National Science Council of Taiwan for financial support of this research.

**Supporting Information Available:** Crystallographic data in CIF format for **1**· $\frac{1}{2}\text{CH}_2\text{Cl}_2$ · $2\text{CH}_3\text{OH}$  and **2**· $\text{CH}_2\text{Cl}_2$ · $\text{CH}_3\text{OH}$ · $4\text{H}_2\text{O}$  and  $^1\text{H}$  NMR and FAB-MS spectra of TBim, TDMBim, **1**, and **2**. This material is available free of charge via the Internet at <http://pubs.acs.org>.

IC800883X

(38) (a) Khlobystov, A. N.; Blake, A. J.; Champness, N. R.; Lemenovskii, D. A.; Majouga, A. G.; Zyk, N. V.; Schröder, M. *Coord. Chem. Rev.* **2001**, 222, 155. (b) Provent, C.; Rivara-Minten, E.; Hewage, S.; Brunner, G.; Williams, A. F. *Chem.—Eur. J.* **1999**, 5, 3487.